Synchrotron x-ray-scattering studies on the sodium dodecyl sulfate–water–pentanol–dodecane L_3 sponge phase

Ning Lei,[1,2,3,*] C. R. Safinya,[3] D. Roux,[4] and K. S. Liang[1]

[1]*Corporate Research Laboratory, Exxon Research and Engineering Company, Annandale, New Jersey 08801*

[2]*Physics Department, Rutgers, The State University of New Jersey, Piscataway, New Jersey 08855*

[3]*Materials Department, Physics Department, Biochemistry and Molecular Biology Program, University of California, Santa Barbara, California 93106*

[4]*Centre de Recherche Paul-Pascal, Domaine Universitaire, 33405 Talence Cedex, France*

(Received 21 November 1995; revised manuscript received 22 November 1996)

High-resolution small-angle x-ray-scattering (SAXS) data in the quaternary sodium dodecyl sulfate–water–pentanol–dodecane membrane system in the L_3 phase were collected and analyzed. The SAXS data show a broad peak followed by q^{-2} and q^{-4} regions at higher q. The data are described quantitatively by the product of a structure factor of $1+C_1\arctan(q\xi_1/2)/q+C_2/[1/\xi_2^2+(|q|-q_c)^2]$ and a form factor of a randomly oriented disks. The C_1 term is the structure factor develop by Cates *et al.* [Europhys. Lett. **5**, 733 (1988)], describing a bicontinuous phase with randomly connected bilayer sheets separating the space at length scales larger than the typical cell size L. The C_2 term, introduced because of the observation of the broad peak centered around q_c in the SAXS data, describes the bilayer cell-cell correlations. For high dilution samples, the form factor alone can describe the data very well. From our data of the water layer volume fraction and $L=2\pi/q_c$, we have determined that for every volume of $(2\pi/q_c)^3$, the membrane has an area of $(1.3–1.8)(2\pi/q_c)^2$. This is consistent with a bicontinuous structure for the L_3 membrane system. The logarithmic increase of the water layer area with $2\pi/q_c$ is due to the membrane thermal undulations. The bending rigidity of the membrane has been found to be $(1.0\pm0.2)k_BT$. [S1063-651X(96)08807-1]

PACS number(s): 82.70.−y, 82.60.−s, 61.30.−v

In many surfactant-cosurfactant solutions, a flow birefringent isotropic phase L_3 has been observed [1–3]. The material in the L_3 phase is transparent and flows easily, in contrast to the very viscous property of the material in the nearby lamellar fluid membrane L_α phase [4]. Based on neutron-scattering data and electric conductivity measurement, Porte *et al.* [17] proposed that the L_3 phase in the cetylpyridinium chloride-brine-hexanol system possessed a flexible spongelike structure, with surfactant bilayers separating the brine into two regions, each of which is connected by itself (see Fig. 1). In addition, freeze fracture electron microscopies on several other L_3 systems carried out by Strey *et al.* [5], revealed a randomly connected bilayer sheet separating the space, which is consistent with the idea of Porte *et al.* [17]. Besides the work of Porte *et al.* [17], a theoretical study by Cates *et al.* [6], also suggested the bicontinuous structure for the L_3 phase. In order to further elucidate the structure and the thermal undulations of the membranes in the L_3 phase, we carried out a high-resolution synchrotron-based small-angle x-ray-scattering (SAXS) experiment on the sodium dodecyl sulfate (SDS)–water–pentanol–dodecane [7] L_3 system. The phase diagram [4] is shown in Fig. 1. The analysis of the SAXS data shows clearly that in this L_3 membrane system, randomly connected SDS-water-SDS bilayer sheets separate dodecane, with a typical cell size L (Fig. 1).

Sodium dodecyl sulfate ($C_{12}H_{25}OSO_3Na$), pentanol, and dodecane were purchased from SIGMA with 99% purity and used without further purification. Deionized water with electric resistivity of 16 MΩ cm was used in this experiment. The weight ratio of water to SDS was kept at 1.552 ± 0.002. The compositions of the samples are listed in Table I.

In the process of making the samples, we found that the higher the dodecane dilution, the faster the equilibrium state is reached. Typically, at about 23 °C, it took a few days for a sample of low dodecane dilution to reach an equilibrium state. For a sample with dodecane concentration larger than 80%, it took only 3–5 h to reach a uniform phase. We have also observed that for higher dodecane diluted samples, it is very easy to produce flow birefringence by shaking the sample. However, the flow birefringence is not observed for the 49.1% docecane diluted sample.

The synchrotron x-ray-scattering experiment was carried out on the Exxon beam line X-10A at the National Synchrotron Light Source (NSLS). Figure 2 demonstrates the experimental setup. To setup a high-resolution small-angle x-ray-scattering experiment, we used a double-bounce Si(111) crystal as the monochromator and a triple-bounce Ge(111) in the nondispersive configuration at small angles as the analyzer. This setup gives an in-plane resolution width of 0.000 18 $Å^{-1}$ [half-width at half maximum (HWHM)] and an out-of-plane resolution width of 0.003 $Å^{-1}$ (HWHM).

The basic features of the scattering from our L_3 samples are shown in Fig. 3, which gives, in logarithmic scale on both axes, the raw data from five samples. We can clearly

*Present address: The Department of Chemistry and the James Franck Institute, The University of Chicago, 5640 Ellis Avenue, Chicago, IL 60637.

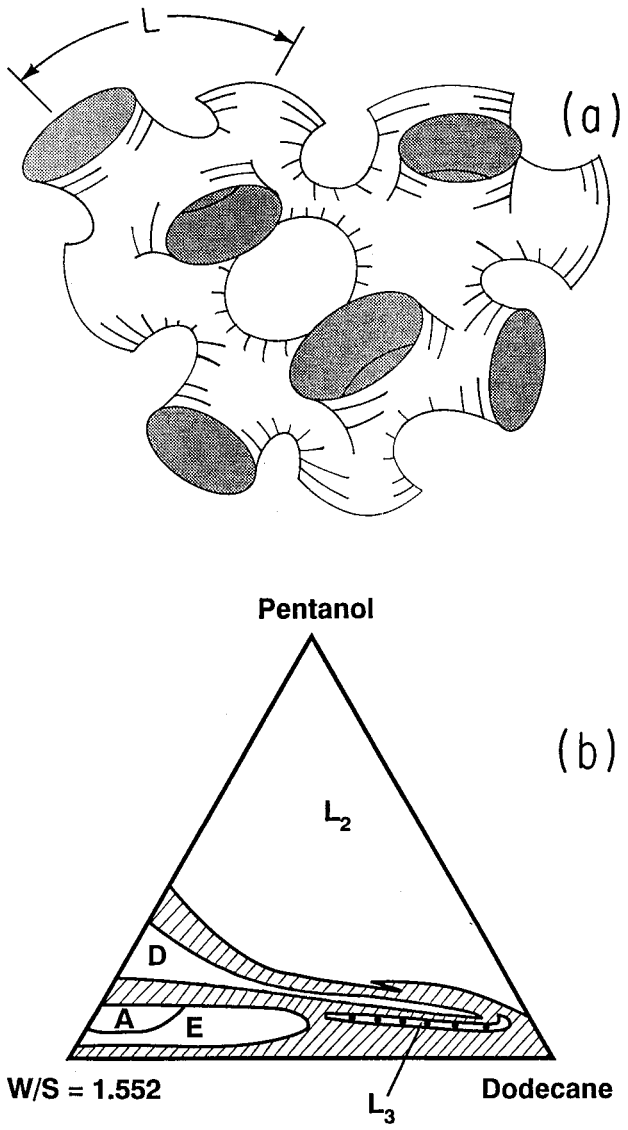

FIG. 1. (a) A sketch of the L_3 sponge phase [redraw from P. Snabre and G. Porte, Europhys. Lett. 13, 641 (1990)]; (b) phase diagram of the quaternary system showing the L_3 sponge phase.

see that most of the curves, corresponding to relatively low dodecane dilutions, have a broad peak denoted as q_c and for a higher dilution sample, although a peak is not obvious, we can still locate a position q_c at which the absolute curvature of the data is of the maximum. At larger momentum transfer q, all the curves show $q^{-2}-q^{-4}$ behavior, although this region is modified by the background scattering, and in the 49.1% dilution case also by the structure factor. The $q^{-2}-q^{-4}$ behavior is characteristic of the scattering from randomly oriented disks [8], indicating that the local structure of our sample is that of flat membranes immersed in dodecane. The evolution of the peak position and its width with the dodecane weight ratio, indicates that with increasing dodecane dilution the cell size L of the membranes increases (i.e., q_c gets smaller) and the cell-cell correlation becomes weaker.

In order to reveal the structure in a quantitative way, we fit the scattering data, by following the theoretical work of Roux *et al.* [2,9], where the L_3 phase was assumed to be

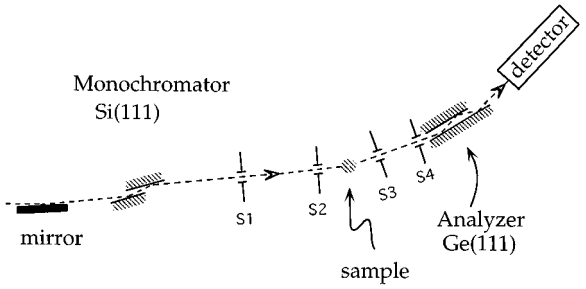

FIG. 2. Sketch of the experimental setup at the Exxon beam line X-10A as described in the text.

comprised of an interconnected infinite sheet separating the space into two regions (in our case it is the SDS-water-SDS bilayer sheet separating dodecane). The regions could be labeled as inside and outside the sheet. The volume difference of the inside and outside creates an in-out order parameter. Considering this order parameter and the sheet volume concentration in the Hamiltonian, the scattering structure factor at a length scale much larger than the cell size has been calculated to be [2,9]

$$C_1 \frac{\arctan(q\xi_1/2)}{q} + 1. \tag{1}$$

Here, ξ_1 is the correlation length associated with the in-out order parameter. To account for the broad peak, the total structure factor might be written as

$$1 + \frac{C_1 \arctan(q\xi_1/2)}{q} + \frac{C_2}{1/\xi_2^2 + (|q| - q_c)^2}. \tag{2}$$

This new C_2 term describes the cell-cell correlation with correlation length ξ_2 and an average cell-cell distance $L = 2\pi/q_c$.

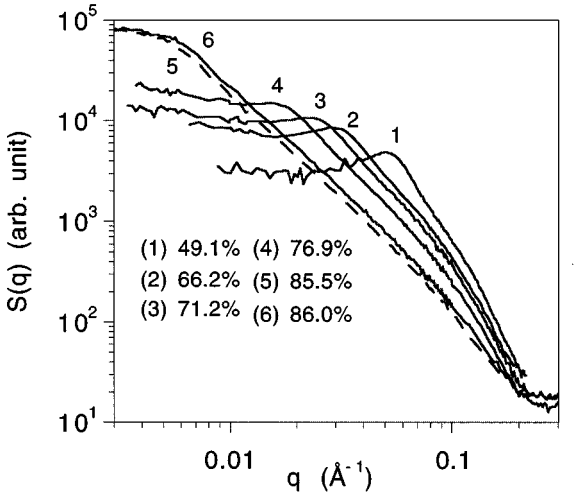

FIG. 3. X-ray scattering data on six samples in the L_3 phase. Let x be the dodecane concentration. The figure shows (1) $x = 49.1\%$; (2) $x = 66.2\%$; (3) $x = 71.2\%$; (4) $x = 76.9\%$; (5) $x = 85.5\%$; and (6) $x = 86.13\%$.

TABLE I. The compositions of the samples in the L_3 phase, with the weight ratio of water to SDS to be 1.552 ± 0.002. In this table, we also list the fitting results. $L \equiv 2\pi/q_c$, with q_c obtained from the data directly, other than from the fit. Solving the linear equations of (detected intensity)=(intrinsic intensity) convoluted with (spectrometer resolution), we have obtained the intrinsic scattering intensities for the samples of dodecane concentrations of 49.1%, 66.2%, 71.2%, 76.9%, 80.0%, and 86.13%. The intrinsic scattering intensities thus obtained are essentially the same as the detected intensities, except at very small q $(<q_c)$.

pentanol %	dodecane %	L (Å)	R (Å)	w (Å)	$1/\phi_\omega$	α
11.2	49.1	125.6±0.2	21.04	25.5	4.839	1.44
10.3	60.0	166.7±0.4	22.8	24.2	6.696	1.38
9.6	66.2	218.0±0.9	25.6	25.4	8.356	1.45
9.4	71.2	277.0±1.8	59.2	25.9	10.60	1.45
8.95	76.9	417.5±3.7	96.0	25.9	14.72	1.58
9.0	80.0	537.9±5.1	127.8	26.0	19.19	1.58
9.0	82.0	658.4±27.6			23.60	1.55
9.0	84.0	898±128			30.52	1.63
9.0	86.13	1177±69	309.2	25.4	43.98	1.49
9.73	85.5	1347±63			44.78	1.67
9.69	85.84	1381±106			47.78	1.61
9.64	86.18	1595±60			51.26	1.73
9.60	86.5	1609±48			48.3	1.61

For the form factor, stimulated by the scattering data, we use that of randomly oriented disks with radius R and thickness w, which is

$$\int_0^1 \left(\frac{J_1(qR\sqrt{1-x^2})}{qR\sqrt{1-x^2}} \right)^2 \left(\frac{\sin(qwx/2)}{qwx/2} \right)^2 dx, \qquad (3)$$

where J_1 is the well-known first-order Bessel function and x is simply the cosine of the orientational angle. A justification to choose such a form factor is that the scattering intensity from a spherical shell of radius R_0 can be represented by that of randomly oriented disks with a suitable choice of R $(=\gamma R_0$, with $\gamma \sim 0.8)$, as demonstrated by Fig. 4. We expect that $R/(2\pi/q_c)$ is roughly a constant at large dodecane dilutions when the membrane thickness is much smaller than the cell size.

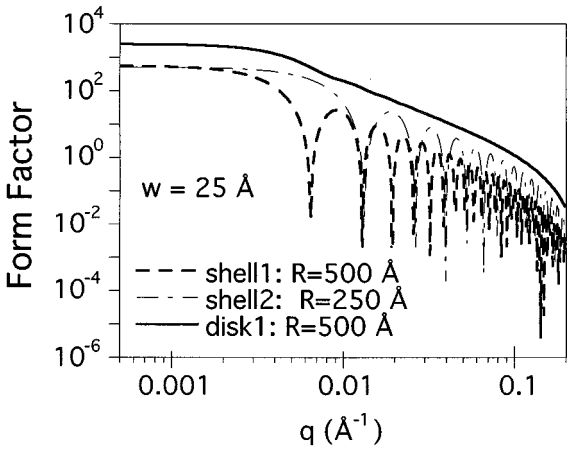

FIG. 4. The solid line shows the form factor from randomly oriented disks with thickness 25 Å and radius 500 Å. The dashed lines show the form factors of spherical shells with thickness 25 Å and radii 250 Å and 500 Å, respectively, as indicated in the figure. If we take the spectrometer resolutions or the spherical shell size distribution into account, the form factor of a suitable spherical shell (or of some size distribution) can be very close to that of randomly oriented disks.

The solid lines in Fig. 5 are the best fits to the experimental data from a few samples in the L_3 phase covering nearly the entire dodecane dilutions, by using Eqs. (2) and (3), convoluted with the spectrometer resolutions. The figure shows that the predictions of the scattering intensity are in good agreement with the data. The fits to the data from other samples are also very good. The good fits suggest that the L_3 phase is of randomly oriented sheets at length scales smaller than the cell size and at length scales larger than the cell size the structure is of an interconnected infinite sheet separating dodecane. The values of the parameters obtained from the fits are listed in Table I.

For samples of large dodecane dilutions (dilution greater than 80.0%), such as 86.13%, the structure factor is practically one and the form factor alone can fit the data satisfactorily. From the fits we know that when the dodecane dilution gets larger, the larger the area of the local flatness becomes, as shown by the evolution of the value of R.

The thickness of the scattering layer is obtained to be roughly the same for all the samples, which is $w=25.5 \pm 0.5$ Å. This value for w is in good agreement with the values obtained elsewhere [4,10,11]. Subtracting the height of the head group of SDS, which is OSO_3, and about 3 Å [12], the water layer thickness is then 19.5 ± 0.5 Å, which is 1.5 Å larger than the value obtained for the membrane system in the nearby L_α phase as shown in Ref. [11]. We believe that this difference is due to the aging SDS sample. The SDS sample had been used many times and absorbed much moisture and therefore we get a larger water layer thickness than that obtained in Ref. [11], where a newly bought SDS sample was used.

We are able to obtain the value of the membrane bending curvature modulus, by using the work of Cates and his colleagues [6], which shows that the L_3 phase has its largest cell size when the membrane persistent length [13] ξ_p is about π/q_c. In our case, we have $\xi_p \approx 1609/2$ Å. Using the well-known formula [13,14]

$$\xi_p = a e^{4\pi\kappa/3k_BT}, \tag{4}$$

we obtain $\kappa = 1.2k_BT$, which is close to its value in the nearby lamellar phase [4,11,15,16]. In Eq. (4), a is a microscopic length, about the nearest surfactant-surfactant distance, which is about 5.7 Å [11]. κ is the bending curvature modulus of the SDS bilayer, k_B is the Boltzmann constant, and T is the sample temperature (~ 300 K).

We do not have data at very small q, so ξ_1 is practically undetectable and enters Eq. (2) as an infinite value for nearly all the samples. Therefore, we cannot obtain $I(q=0)$ for nearly all the samples and check the consistency with the predicted behavior [2,3,9]

$$1/I(q=0) \propto \phi_w \ln(\phi_w/\phi_*).$$

A useful way to determine the membrane structure of our samples at length scales of the cell size is to use the work of Porte *et al.* [17], which relates $2\pi/q_c \equiv L$ [17,18] with sheet thickness δ_0. Porte *et al.* pointed out that for structures formed by sheets, the following relation holds:

$$\frac{2\pi}{q_c} = \alpha \frac{\delta_0}{\phi_w}, \tag{5}$$

where ϕ_w is the sheet volume fraction and in our case we set it equal to the water volume fraction. For lamellar structures without ripples, α is equal to 1 and for bicontinuous structures without ripples α is about 1.5 [17].

When considering the thermal ripples on the membranes, α in Eq. (5) is not independent of the cell size any more. In this case, Eq. (5) is modified to be

$$\frac{2\pi}{q_c} = \alpha_0 \frac{\delta_0}{\phi_w}\left[1 + \frac{k_BT}{4\pi\kappa}\ln\left(\alpha_0 \frac{\delta_0}{c\phi_w}\right)\right], \tag{6}$$

where c is a numerical factor. Equation (6) says that the volume of the membrane sheet increases when considering the thermal ripples and the ripples considered are from the thermal undulations of a piece of membrane of size L/c. We take c as 10 and the reason for choosing such a large factor is that for large ripples of the size of L, the extra sheet volume is accounted for by α_0, since such ripples actually relate to the overall shape of the membranes. Furthermore, if we took c as a relatively small factor such as 2, then the size of the membrane responsible for the ripples is so large that the membrane tilt angle is not small and therefore our formalism breaks down. Besides, as demonstrated by the fitting results, the smaller c is, the smaller α_0 is, indicating that the membrane fluctuation at large length scales is a big contribution to α_0 (see the fitting results for different c in Ref. [22]). Therefore, if we want α_0 to account for the membrane shape at large length scales, we need to choose c to be much larger than 1.

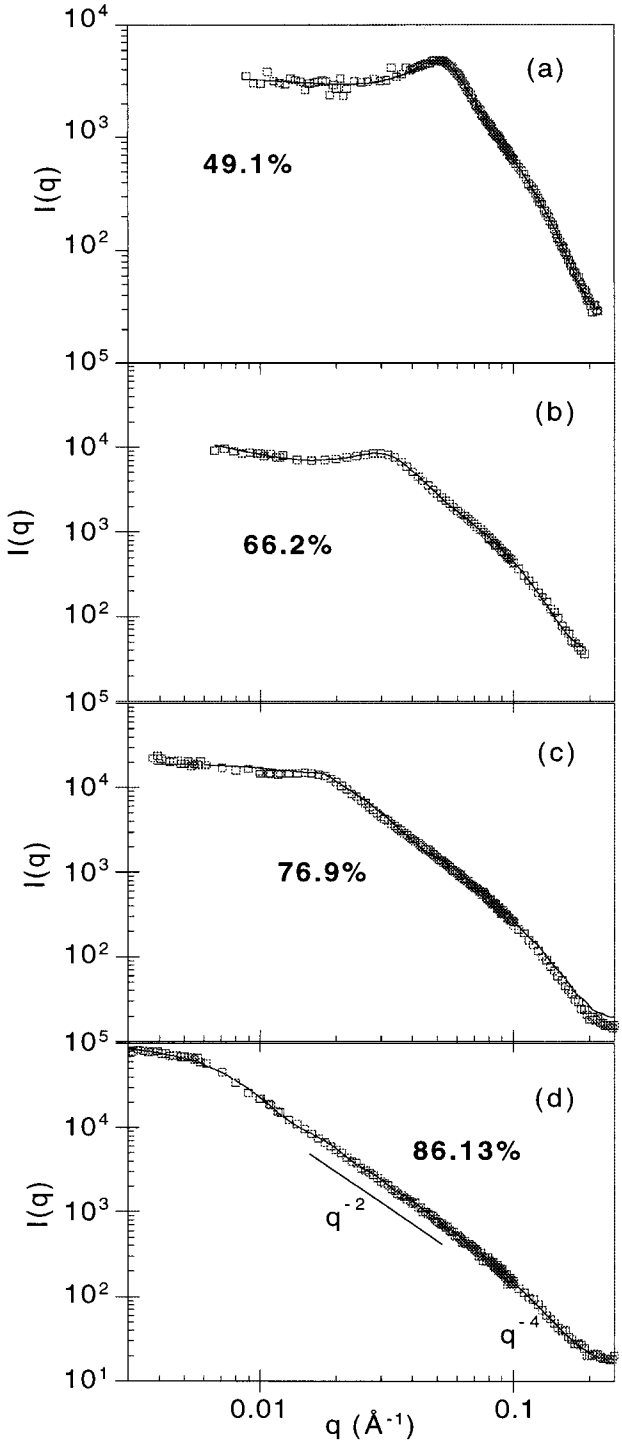

FIG. 5. Best fits of scattering data from four samples to the product of Eqs. (2) and (3), with an overall scale factor, which is unimportant for the issues in this paper. Solid lines are the fits and the squares are the data. The slope variation at $q \sim 0.1$ Å^{-1} is due to the thickness of the scattering layer w.

Now we need to know the water volume fraction ϕ_w. As demonstrated before [19], within a relative error of less than 0.005, the water volume fraction can be calculated by

$$\phi_w=\frac{\frac{1.552}{2.552}(1-x_{\rm dod}-x_{\rm pen})/0.998\ 23}{\frac{1.552}{2.552}(1-x_{\rm dod}-x_{\rm pen})/0.998\ 23+\frac{1.0}{2.552}(1-x_{\rm dod}-x_{\rm pen})/\rho_{\rm SDS}+\frac{x_{\rm dod}}{\rho_{\rm dod}}+\frac{x_{\rm pen}}{\rho_{\rm pen}}}, \tag{7}$$

where $x_{\rm dod}$,$x_{\rm pen}$ are the weight percentages for dodecane and pentanol, and $\rho_{\rm SDS}=1.168$ g/cm^3, $\rho_{\rm pen}=0.8144$ g/cm^3, and $\rho_{\rm dod}=0.7487$ g/cm^3, are the mass densities for SDS, pentanol and dodecane at 20 °C, respectively. The water mass density at 20 °C is 0.998 23 g/cm^3 [20]. The thermal expansion coefficients for all the materials are about 1×10^{-4} [21] and, therefore, at a slightly higher temperature of a few degrees above 20 °C the density values at 20 °C can still be used in Eq. (7) to generate accurate results. Note that $1.552(1-x_{\rm dod}-x_{\rm pen})/2.552$ is the weight of water in one unit weight of the sample. Therefore, the numerator is the volume of the water and the denominator is the total volume, in one unit weight of the sample. The water volume fractions calculated by Eq. (7) are listed in Table I.

In Fig. 6 we plot $2\pi/q_c$ vs $1/\phi_w$. The dashed line in the figure is the best fit to the old formula Eq. (5), which yields $\alpha=1.43\pm0.04$, if we take $\delta_0=18$ Å [11]. Obviously, the dashed line misses the data points substantially at high dodecane dilutions. A better fit is the solid line which is the best fit to our new formula Eq. (6). The fit yields $\alpha_0=1.40\pm0.04$ [22] and $\kappa=(3.0\pm2.8)k_BT$. The value of α_0 obtained agrees with what is expected for an interconnected membrane structure. The value of κ obtained from the fitting possesses a large statistical error, due to the large errors in $2\pi/q_c$ determinations at higher dodecane dilutions.

A better way to obtain the value of κ comes from rewriting Eq. (5) as

$$\alpha=\frac{\phi_w L^3/\delta_0}{L^2}\equiv\frac{\phi_w L}{\delta_0}. \tag{8}$$

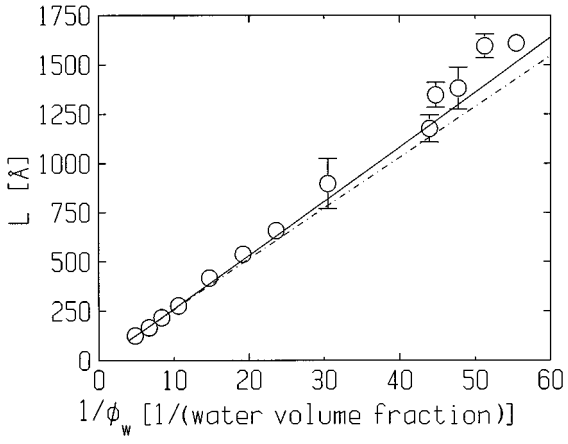

FIG. 6. Plot of $L\equiv2\pi/q_c$ vs $1/\phi_w$ and the best fits to Eq. (5) (dashed line) and Eq. (6) (solid line), respectively. The dashed line corresponds to $\alpha=1.43\pm0.04$ and the solid line corresponds to $\alpha_0=1.40\pm0.04$ and $\kappa=(3.0\pm2.8)k_BT$. q_c is scattering peak position and is obtained from the data directly, other than from the fit. ϕ_w is the water volume fraction for the sample and is calculated through Eq. (7). Error bars are estimated from the data and shown in the bars.

$\phi_w L^3/\delta_0$ is just the water layer area in one unit cell. The values of α as calculated by Eq. (8) are in the range of 1.3–1.8, consistent with the spongelike membrane structure. We list the values of α, as calculated by Eq. (8), in Table I. In Fig. 7 we plot α vs L and it is obvious to see that α monotonically increases with the cell size. A fit of the data (α,L) to

$$\alpha=\alpha_0\left[1+\frac{k_BT}{4\pi\kappa}\ln\left(\frac{L}{10}\right)\right] \tag{9}$$

gives $\alpha_0=1.32\pm0.03$ and $\kappa=(1.0\pm0.2)k_BT$. The solid line in Fig. 7 is the best fit. The reason for the smaller error bar in the κ determination is that Eq. (8) yields a relatively smaller error bar at large L, because at large L, ϕ_w is smaller.

In conclusion, we have carried out a small-angle x-ray-scattering experiment in the quaternary SDS–water–dodecane–pentanol membrane system in the L_3 phase. Our data are consistent with the L_3 phase being a spongelike, symmetric bicontinuous structure with a locally flat SDS bilayer sheet separating dodecane. The membrane bending rigidity is obtained to be $(1.0\pm0.2)k_BT$.

We point out that among the very dilute phases which appear at equilibrium in surfactant solutions, the lamellar L_α phases that are stabilized by the Helfrich undulation forces [4,10,15,23] and the sponge L_3 phases are now essentially understood both theoretically and experimentally. In contrast, a recently discovered equilibrium dilute phase of surfactant solutions is far from being understood [24]. This discovery shows a new phase of liposomes, not predicted by current theories describing fluid membranes, consisting of an equilibrium multilamellar tubular vesicles (L_{tv}) in membranes with bending rigidity of order k_BT. Recent theoretical work which emphasizes a nonanalytical bending energy term

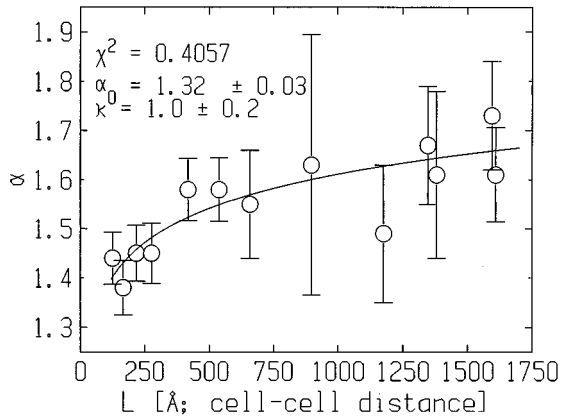

FIG. 7. Data of (α,L) and the best fit to Eq. (9). α is defined by Eq. (5) and obtained by Eq. (8). The fit yields $\alpha_0=1.32\pm0.03$ and $\kappa=(1.0\pm0.2)k_BT$.

that appears to favor cylindrical and ''egg-carton'' geometries [25] and maybe relevant to the L_{tv} phase observation.

Our understanding on the L_3 phase has benefited from discussions with Scott Milner and Sunil Sinha. We thank S. Bennet and J. Marsh for technical support. C.R.S. gratefully acknowledges partial support from NSF, under Grant No. DMR-9624091, and the Petroleum Research Fund (Grant No. 31352-AC7). NSLS is supported by the U.S. Department of Energy.

[1] P. G. de Gennes, Rev. Mod. Phys. **64**, 645 (1992).
[2] D. Roux and C. Coulon, J. Phys. Chem. **96**, 4174 (1992).
[3] G. Porte, M. Delsanti, I. Billard, M. Skouri, J. Appell, J. Marignan, F. Debeauvais, J. Phys. II **I**, 1101 (1991).
[4] C. R. Safinya, D. Roux, G. S. Smith, S. K. Sinha, P. Dimon, and N. A. Clark, Phys. Rev. Lett. **57**, 2718 (1986); C. R. Safinya, in *Phase Transitions in Soft Condensed Matter*, edited by T. Riste and D. Sherrington (Plenum, New York, 1989).
[5] R. Strey, W. Jahn, G. Porte, and P. Bassereau, Langmuir **6**, 1635 (1990).
[6] M. E. Cates, D. Roux, D. Andelman, S. T. Milner, and S. A. Safran, Europhys. Lett. **5**, 733 (1988).
[7] We later noticed that Gazeau *et al.* had carried out a neutron scattering experiment and an electric conductivity measurement on the same membrane system; see D. Gazeau, A. M. Bellocq, D. Roux, and T. Zemb, Europhys. Lett. **9**, 447 (1989).
[8] C. F. Schimidt, K. Svoboda, Ning Lei, I. Petsche, L. Berman, C. R. Safinya, and G. Grest, Science **259**, 952 (1993).
[9] D. Roux, M. E. Cates, U. Olsson, R. C. Ball, F. Nallet, and A. M. Bellocq, Europhys. Lett. **11**, 229 (1990).
[10] D. Roux and C. R. Safinya, J. Phys. (France) **49**, 307 (1988).
[11] Ning Lei (unpublished).
[12] F. A. Cotton and G. Wilkinson, *Advanced Inorganic Chemistry* (Wiley, New York, 1988).
[13] P. G. de Gennes and C. Taupin, J. Phys. Chem. **86**, 2294 (1982).
[14] L. Peliti and S. Leibler, Phys. Rev. Lett. **54**, 1690 (1985).
[15] Ning Lei, C. R. Safinya, and R. F. Bruinsma, J. Phys. II **5**, 1155 (1995).
[16] F. Nallet, D. Roux, and J. Prost, Phys. Rev. Lett. **62**, 276 (1989).
[17] G. Porte, J. Marignan, P. Bassereau, and R. May, J. Phys. (France) **49**, 511 (1988); G. Porte, J. Appell, P. Bassereau, and J. Marignan, *ibid.* **50**, 1335 (1989).
[18] J. P. Hansen and I. R. McDonald, *Theory of Simple Liquids* (Academic, New York, 1986).
[19] Ning Lei (unpublished).
[20] *CRC Handbook of Chemistry and Physics*, edited by R. C. Weast (CRC, Boca Raton, FL, 1990).
[21] *Handbook of Physical Calculations*, edited by J. J. Tuma (McGraw-Hill, New York, 1976).
[22] If we take $c=4$, then we get $\alpha_0=1.23\pm0.05$ and $\kappa=(1.0\pm0.2)k_BT$ and if we take $c=40$, we get $\alpha_0=1.46\pm0.02$ and $\kappa=(1.2\pm0.2)k_BT$. The fitting χ^2 are the same. So we can see that the value of κ does not differ much over a reasonable range of c.
[23] W. Helfrich, Z. Naturforsch. C **28**, 693 (1973); Z. Naturforsch. A **33**, 305 (1978).
[24] S. Chiruvolu, H. E. Warriner, E. Naranjo, K. Kraiser, S. H. J. Idziak, J. Radler, R. J. Plano, J. A. Zasadzinski, and C. R. Safinya, Science **266**, 1222 (1994).
[25] J. B. Fournier, Phys. Rev. Lett. **76**, 4436 (1996).